RSC Advances

ROYAL SOCIETY OF CHEMISTRY

www.rsc.org/advances

β-$NiMoO_4$ nanowire arrays grown on carbon cloth for 3D solid asymmetry supercapacitor

Chuanshen Wang, Yi Xi,* Chenguo Hu, Shuge Dai, Mingjun Wang, Lu Cheng, Weina Xu, Guo Wang and Wenlong Li

Department of Applied Physics, Chongqing University, Chongqing, 400044, China

Abstract

Based on β-$NiMoO_4$ nanowire(NW) arrays grown on carbon cloth as the electrode materials, the 3D solid asymmetry supercapacitor has been fabricated. The produced β-$NiMoO_4$ NW arrays compared to film of power can increase the efficiency of nanomaterials participated in reactions. The cone-shape NW arrays have high specific surface area (99 m^2/g), which can provide more electroactive sites for Li^+ and enhance conductivity through providing short transport and diffusion path for both ions and electrons. And the cylinder supercapacitor can make more β-$NiMoO_4$ NW arrays saturate with electrolyte to enhance the property of supercapacitor. Furthermore, the electrode gets the highest energy density of 36.86 Wh/kg, the maximum power density of 1100 W/kg, and large capacitance of 414.7 F/g at the current density of 0.25 A/g, all of which exhibit excellent behavior. And the stability of supercapacitor reached 65.96 % of initial capacitance over 6000 times. All these results indicated that the β-$NiMoO_4$ NW arrays grown on carbon cloth could be a promising candidate for high performance supercapacitors.

* Corresponding author
Tel +86 23 65678362 Fax +86 23 65678362 *E-mail addressed* yxi6@cqu.edu.cn (Y Xi)

Keywords: β-$NiMoO_4$, 3D nanostructure, solid, supercapacitor

1. Introduction

With the proliferation of electronic devices, the requirement for property of portable power supplies is becoming evidently increasing. Energy storage devices such as batteries, supercapacitors are an indispensable part of our current society[1,2]. Supercapacitors, also named as electrochemical capacitors (ECs) or ultra-capacitors, afford a very promising for energy storage application for its advantages, which have long cycle life, high power density, long standing time, environment friendless, safety and so on. Supercapacitors can be classified into two varies, according to its storage mechanisms[3,4], electrical double layer capacitors (EDLCs) and pseudo-capacitors[5,6]. These two mechanisms can function simultaneously relying on the nature of the electrode materials. In general, carbon materials, because of its high specific area, are applied in EDLCs. Conducting polymers and metal oxides are used for pseudocapacitors[7-9]. To obtain high power density and cycling stability, the appropriate nanomaterials are essential[10-12]. Moreover, supercapacitors have proper property and flexibility, which can meet various design and power needs of modern gadgets[13,14]. At the same time, according to the energy density (E) of supercapacitors, its equation can be given as follows: $E=1\backslash 2\ CV^2$. The way of enhancing its capacitance are developing novel electrode materials or expanding the potential window[15,16]. Due to metal oxide's special capacitive properties of higher capacitance than most of conductive polymers, considerable research efforts have been focused on developing metal oxide materials. Metal oxide materials can be divided into three categories. (a) single metal oxides NiO, Co_3O_4, MnO_2, RuO_2, etc[17-20]. (b) binary metal oxides, such as $NiCo_3O_4$, $NiMoO_4$, $CoMoO_4$, etc[21-23]. (c) hybrid nanostructure, such as Co_3O_4@$NiMoO_4$, $NiCo_3O_4$@MnO_2, MnO_2/KCu_7S_4, etc[24-26]. Nickel molybdates ($NiMoO_4$) crystalline has three polymorphic forms, two of them, α and β are stable in standard pressure condition. α- $NiMoO_4$ and β- $NiMoO_4$ are both monoclinic but have different Mo coordination, that is to say, they have octahedral and tetrahedral sites, respectively[27-29]. Naocrystalline $NiMoO_4$ has lots of advantages, such as short diffusion path lengths, pseudocapacitive contributions to charge storage, and the stability of the materials to more easily accommodate the strains from lithium intercalation[28]. Furthermore, based on $NiMoO_4$ nanowire (NW) arrays grown on carbon cloth, it has the good electrical conductivity, low-cost, flexible and large specific surface. So based on $NiMoO_4$ NW arrays grown on carbon cloth are candidate electrode materials for its good electrochemical property[29].

In our work, based on $NiMoO_4$ NW arrays grown on carbon cloth, we report the high performance 3D all-solid-state cylinder supercapacitor is different from the reported liquid supercapacitor[30]. The β-$NiMoO_4$ NW arrays which had grown on carbon cloth electrode display a wide potential window, high power density and good

cycle stability for supercapacitor. This kind of supercapacitor is the asymmetry cylinder, which consists of the cathode of the β-$NiMoO_4$ NW arrays gown on carbon cloth and the anode of the β-$NiMoO_4$ NW arrays gown on carbon wires twisted on carbon rod. Furthermore, the supercapacitor can power one light-emitting diode (LED) about 260 seconds. This type of supercapacitor is solid-supercapacitor, which will overcome the major disadvantages of conventional liquid supercapacitor. It is pivotal for device integration and environmental friendless. All this research indicates the β-$NiMoO_4$ NW arrays are idea materials for supercapcaitor electrode materials, and the all-solid-state asymmetry cylinder supercapacitor has excellent capacitance performance.

2. Experimental Section

2.1. Synthesis of β-$NiMoO_4$ NW arrays on carbon cloth

The approach of β-$NiMO_4$ NW arrays synthesis on carbon cloth is a facile hydrothermal method, which is a minor different from the literature[31]. The reagents without further purification in the experiment were all analytical grade. Prior to the synthesis, the carbon cloth substrate length × width = 2 cm × 3 cm and carbon fiber were rinsed with ammonia water (PH=7) and water respectively. The washed carbon cloth and carbon fiber dried in an oven for 30 minutes and was immersed in the 5% $KMnO_4$ solution for 40 minutes. Then it was placed in the Teflon-lined autoclave. 2.5 mmol of Ni $(NO_3)_2 \cdot 6H_2O$ and 2.5 mmol of $Na_2MoO_4 \cdot 2H_2O$ was mixed in 50 ml ultra pure water under constant magnetic stirring until they became clear. The mixture solution was transferred into Teflon-lined stainless steel autoclave liners and the treated carbon cloth and carbon fiber were immersed into the mixture solution. The mixture solution was divided into three parts at above same condition. They all were sealed into Teflon-lined stainless steel autoclave liners and maintained at 100 ℃, 140 ℃ and 180 ℃ for 8 hours (h). After cooling down to room temperate, the carbon cloth which had a very light green precipitate was taken out and washed with distilled water and alcohol by ultra-sonication. When all the residual nanoparticles were removed, the carbon cloth was dried at 55 ℃ for 5 h and annealed at 450 ℃ for 2 h in air. Above procedures were repeated besides the temperature was set at 140 ℃ for 5, 8 and 11 h.

2.2 Assembly of the solid-state supercapacitor

The β-$NiMoO_4$ NW arrays 3D suppercapacitor was consisted of β-$NiMoO_4$ NW arrays grown on carbon cloth, a solid electrolyte (polyvinyl alcohol PVA-LiCl gel), separator and the β-$NiMoO_4$ NW arrays gown on carbon fibers twisted on carbon rod (β-$NiMoO_4$ NWs on carbon cloth as the positive electrode and carbon thread as the negative electrode). PVA-LiCl gel electrolyte was reported elsewhere[2]. In the fabrication process, firstly one carbon thread was

textile-wrapped around a carbon rod as negative electrode with about 2 cm in length. Secondly, the electrode was coated with a layer of electrolyte (LiCl-PVA gel), and then was wrapped with a separator (Whatman 8 μm filter paper) which was coated with the electrolyte on both sides. Finally, one piece of carbon cloth (2 cm × 3 cm) which was put electrolyte uniformly was twined with the previous processed electrode for the micro-supercapacitor.

2.3. Characterization and electrochemical measurement

The surface microstructure and morphology of the sample were characterized by a scanning electron microscope (Nova 400 nano SEM) and a transmission electron microscope (TEM, TECNAI20 Philips). The specific surface area was measured by the multipoint Brunauer-emmett-teller (BET) method at 77.3 K with a quantachrome NOVA4200e system. The pore size distribution was also obtained from the desorption isothersm by Barrett–Joyner–Halenda (BJH) method. Energy-dispersive X-ray (EDS) spectroscopic analysis was performed by an INCA, Oxford Instruments attached with SEM. The carbon cloth X-ray diffraction (XRD) was recorded on a BDX 3200 China with CuKα radiation. The cyclic voltammetry (CV) and galvanic charge-discharge (GCD) measurement were conducted using a chemical workstation (CHI760D). The electrochemical impedance spectroscopy (EIS) was carried out in a frequency range of 1-100 kHz at open circuit potential of 0.01 V. Specific capacitances are calculated from the CV and charge-discharge curves by the way of Eq. 1 and Eq. 2, respectively. The area capacitance is as same as Eq. 1 and Eq. 2 besides m is substituted by S. The energy density (E) and power density (P) are calculated according to Eq. 3 and Eq. 4[28-31].

$$C_{m1}=\frac{\int I_1 dV}{\nu m \Delta V} \quad (1)$$

$$C_{m2}=\frac{I_2 \Delta t}{m \Delta V} \quad (2)$$

$$E=\frac{I \Delta t \Delta V}{2m} \quad (3)$$

$$p=\frac{I \Delta V}{2m} \quad (4)$$

Where I_1 is the response current, ΔV is the voltage window, ν is the scan rate, I_2 is the constant discharge current, Δt is the discharging time and S, m is the geometrical area of the ECs and the total mass of the ECs, respectively.

3. Results and discussion

3.1 Material characterization

In this study, a facile hydrothermal approach was used for the synthesis of β-$NiMoO_4$ NW arrays grown on carbon cloth. The details are shown in the experimental part. The schematic illustration for the formation processes of the β-$NiMoO_4$ NW arrays on carbon cloth can be shown in Figure 1. The chemical reaction equations can be listed as

follows[35-37].

$$(1)\quad Ni(NO_3)_2\cdot 6H_2O + Na_2MoO_4\cdot 2H_2O \xrightarrow{140℃} NiMoO_4\cdot xH_2O + 2NaNO_3$$

$$(2)\quad NiMoO_4\cdot xH_2O \xrightarrow{450℃} NiMoO_4 + xH_2O$$

The crystal phase structures and purity of β-$NiMoO_4$ NWs on carbon cloth were investigated by the X-ray diffraction. Figure 2(a) shows XRD patterns of β-$NiMoO_4$ supported on carbon cloth at different time of the same temperature (140 ℃ at 5, 8 and 11 h). The strong peak of XRD is typical peak of β-$NiMoO_4$ products, however, which can not be distinguished from the main peak of carbon cloth. But some inferior peaks ((02-1), (201), (11-2), (31-1), (112), (22-1)) which are in good accordance with the monoclinic structure of β-$NiMoO_4$ (JCPDS-No.45-0142 with space group C2/m (12) and cell parameters a=10.18 Å, b=9.241 Å, c=7.018 Å) can accurately confirm this kind of material[38]. Moreover, the inset of Figure 2(a) suggests the as-prepared β-$NiMoO_4$ has poor crystallinity and the existence of characteristic (11-2) is typical characteristic peak of β-$NiMoO_4$. And the chemical components of the β-$NiMoO_4$ are characterized by energy dispersive EDS as shown in Figure 2(b). The elements are Ni, Mo, O, C and the C is indexed to carbon cloth substrate. The EDS pattern of this material has hardly any noise peaks, which indicates little electric charge effect. That is to say, the conductivity of β-$NiMoO_4$ is well. To identify the existence of β-$NiMoO_4$, the TEM was carried out. From the Figure 2(c), the diameter of β-$NiMoO_4$ arrays was about 27-40 nm. Importantly, the high-resolution TEM of figure 2(d) shows that the interplanar spacing is 0.31 nm and 0.35 nm，corresponding to the (220) and (310) plane of $NiMoO_4$ in the standard PDF number (JCPDS-No.45-0142). The different time (5, 8 and 11 h) SEM of β-$NiMoO_4$ arrays at 140 ℃ have been displayed in Figure 3(a)-(c). The SEM images of β-$NiMoO_4$ arrays on carbon cloth at different temperatures (100, 140 and 180 ℃) were shown in Figure S1(a),Figure 3(b) and (d). Compared with naked carbon cloth (Figure S1(b)), the rod-like structure of β-$NiMoO_4$ NW arrays was grown on the carbon fibers and the Figure 3(b) had uniform structure and more spaces between arrays than Figure 3(a) and 3(d). From these results, we can see that the prior grown conditions are the grown time 8 h at 140 ℃. Meanwhile, nitrogen adsorption-desorption revealed that the specific surface area of the Figure 3(b) is 99 m^2/g, which is higher than 18.438 m^2/g (Figure 3(a)) and 25.361 m^2/g (Figure 3(c)). And the highest specific surface area of the Figure 3(b) is higher than many literatures[39, 40]. And the pore diameter is about 3.73 nm from the analysis of BJH.

3.2 Electrochemical properties

To further manifest excellent behavior of this β-$NiMoO_4$ NW arrays electrode and investigate its potential application in supercapacitor, CV curves, GCD curves, cyclic performance and EIS were performed in a two-electrode solid electro-chemical cell containing the LiCl-PVA gel electrolyte. First, the electrode was fabricated, and the details are shown in the experimental part. Moreover, the loading mass of positive and negative materials is about 0.6 mg/cm^2, 0.23 mg at 140 ℃ for 5 h, 0.62 mg/cm^2, 0.25 mg at 140 ℃ for 8 h and 0.63 mg/cm^2, 0.26 mg at 140 ℃ for 11 h, respectively. The fabrication process of 3D supercapacitor can be shown in Figure 4. CV curves of this electrode with the potential ranging 0 from to 0.8 V were performed at different scan rates, as is shown in Figure 5. Each CV curve is comprised of the quasi rectangular profile, which indicates the idea pseudo-capacitive property of electrode and fast redox reaction with PVA/LiCl under wide range of scan rates[38]. Furthermore, the highest current response up to -0.035 A-0.035 A in the CV curves displays the excellent charges storage ability and quick ion mobility between the electrode and electrolyte. As is shown in Figure 5(d), the EC at the synthesis time of 8 h has highest performance for having biggest specific area. The β-$NiMoO_4$ NW arrays grown on carbon cloth (2 cm × 2 cm) electrode, Pt foil and a standard calomel electrode were used as working electrode, counter electrode and reference electrode, respectively by using three-electrode measurement. Figure S2(a-c) show CV curves of β-$NiMoO_4$ at different scan rates with same time. Figure S2(d) shows the CV curves of β-$NiMoO_4$ at scan rate of 200 mV/S of different as-prepared $NiMoO_4$ grown time. Each CV curve of β-$NiMoO_4$ has the strong redox peaks, indicating the pseudocapacitive characteristics of the as-prepared $NiMoO_4$ electrode material[25, 31]. Lastly, the asymmetric redox peaks suggested the β-$NiMoO_4$ NW arrays electrode materials are unstable.

GCD of $NiMoO_4$ NW arrays supported on carbon cloth ECs (140 ℃ at 5, 8 and 11 h) with different discharge current desities ranging 0.25 A/g to 2.75 A/g, as shown in Figure S3(a-c). Figure 6(a) shows the discharging time at current density of 0.75 A/g (140 ℃ at 8 h) is the longest, which indicates the best performance. Figure 6(b) shows the nearly triangular shape of charge-discharge cycles shows very symmetry and long time linear slope at high discharge current values, which manifest the excellent conductivity and well capacitance. Presented in inset of Figure 6(b), it is observed that the discharging time can reach 42.5 seconds even at the current 2.75 A/g. On the basis of Eq. 2, the specific capacitances of the ECs were calculated to be 414.7, 306.75, 247.03, 204.75, 170.16, 139.22 F/g at current densities of 0.25 A/g, 0.75 A/g, 1.25 g/A, 1.75 A/g, 2.25 A/g and 2.75 A/g, respectively, as shown in Figure 6(c). Although the specific capacitance is much lower than the previous reports of $NiMoO_4$[25, 31, 42] at the same scan rate, the reactions occur in solid electrolyte. Moreover, the specific capacitance of β-$NiMoO_4$ NW arrays on carbon

cloth is very high compared to the specific capacitance of some metal oxide materials[43-45]. The wide range of the scan rates shows the Li^+ of electrolyte has enough time to diffuse between electrolyte and electrode. Form the inset of Figure 3(b), the products have both a robust adhesion and electrical contact to the carbon fibers and a net structure which has lots of interspaces, matching with high specific surface area[31]. The spaces between the NWs and NWs have so many that can make the electrolyte fully accessible. So the main reasons might be due to the higher porous structure of β-$NiMoO_4$ NW arrays for easy diffusion of the electrolyte into the inner region of electrodes and the high conductivity of carbon cloth with multi-channels[41]. Furthermore, the potential drop (IR drop) about 0.03 V at the current density of 0.25 A/g at the beginning of discharging cycle, which indicates fast I-V response and low internal resistance (Rs) of the capacitance. The IR drop can account for Rs of the products or the contact resistance between electrode and electrolyte. Based on Eq. 3 and Eq. 4, the power density (P) and energy density (E) can be further calculated from the GCD curves of Figure 6(b). For the β-$NiMoO_4$ NW supercapacitor, the energy densities were 36.86, 27.27, 21.96, 18.2, 15.13 and 12.3 Wh/kg, and the power densities were 100, 300, 500, 700, 900 and 1100 W/kg , which is displayed in Figure 6(d), respectively.

Due to the $NiMoO_4$ NW arrays were supported on carbon cloth, the electrochemical performances of original carbon cloth were tested. Figure S1(c) and (d) demonstrate CV and GCD curves of the original carbon cloth. And the CV and GCD curves of $NiMoO_4$ NW arrays supported on carbon cloth are displayed in Figure 5(b) and Figure 6(b). Contrasted to the CV and GCD curves of original carbon cloth electrode, the β-$NiMoO_4$ NW arrays electrode is far better than it. The reason is that the special structure of supercapacitor and lots of mesopores of β-$NiMoO_4$ guarantee sufficient β-$NiMoO_4$ NW arrays supported on carbon cloth participating in enhancing capacitance of supercapacitor. It is essential for practical, flexible, lightweight, portable and environmental friendless devices. The 3D supercapacitor of β-$NiMoO_4$ NW arrays is the flexible and can be winded at two-dimension plane. Furthermore, it is assumed that if the carbon rod is replaced by bronze rod, the supercapacitor will be curved at any angle without destroying its physical structure.

It is important to investigate the long term cycle stability on this kind of supercapacitor. The stability of supercapacitor has been studied by repeating the charge-discharge process at the potential ranging from 0 to 0.8 V. From the Figure 7, the columbic efficiency is nearly 100 % for every charge-discharge cycle. The value of specific capacitance is calculated with respect to the number of charge-discharge cycles at constant 6 A/g. The capacitance of first 800 cycles decreased about 5.3 % and it increased at the beginning of 800st until at the end of 2000th. The

capacitance decreased with the cycle numbers and got 65.9 % retention of initial specific capacitance after 6000 cycles. The bad stability indicated that this material is not suitable enough during the long time test. It is due to the diffusion of ions between electrolyte and active material of the electrode is not very well at high current density.

Figure 8 displays the EIS in the frequency range of 1-100 kHz with open circuit potential of 0.01 V. The measured EIS spectra was analyzed by Nyquist plot and ZSim software simulation method based on the equivalent circuit, which is also displayed in the set of Figure 8(a). The inset Figure 8(a) which shows the enlarged semicircle in a high frequency fit well with the equivalent circle model. In the low frequency range, the line is not vertical. It indicates that the diffusions of ions between electrolyte and active material of the electrode is not very well. This property is in accordance with the cycling stability. The intersecting point with real axis in high frequency region shows Rs of the products contains ionic resistance, inherent resistance of β-$NiMoO_4$ NW arrays and carbon cloth and contact resistance of electrode materials and electrolyte[1]. The Rs of β-$NiMoO_4$ NW arrays grown on carbon cloth is about 3.4 Ω, as is shown in the inset of Figure 8(a). The small semicircle indicates the fine electrical conductivity and small resistance of the material. The behavior of EIS accords with the small IR of GCD curves. The charge transfer resistance (R_f) between electrode and electrolyte is about 1.4 Ω.

For the purpose of investing the electrochemical stability, EIS was performed after finishing 6000 cycles, as is presented in Figure 8(b). Rs of supercapacitor before 6000 cycles showed by the intersecting with real axis in the high frequency region is almost as same as Rs after 6000 cycles. All these prove the electrode materials are grown on carbon cloth have excellent performance. R_f is calculated about 1.4 Ω and 1.5 Ω before and after 6000 cycles, respectively.

Based on all above results, the β-$NiMoO_4$ NW arrays on carbon cloth electrode are promising for supercapacitor application. The high performance of the β-$NiMoO_4$ NW arrays electrode can be listed as follows. First, as is shown in Figure 9(a) and (b), the poor crystallinity which can provide more mesopores and the open space between NWs greatly increase conductivity through providing short transport and diffusion path for both ions and electrons and could provide more electro-active sites for Li^+ [46, 47]. Because the β-$NiMoO_4$ NW arrays were synthesized in relative low temperature and annealed in air. Second, the high capacitance of β-$NiMoO_4$ NW arrays is mainly attributed to the deintercalation/intercalation of Li^+ and reversible redox reaction Ni(Ⅱ)/Ni(Ⅲ)[31,38,48]. The possible reactions deintercalation/intercalation of Li^+ and reversible redox reaction Ni(Ⅱ)/Ni(Ⅲ) can be listed as following.

$$Ni_xMo_{1-x}O_4 + yLi^+ + ye^{-1} \leftrightarrow Li_yNi_xMo_{1-x}O_4 \quad (3)$$

$$Ni_xMo_{1-x}O_4 + 3xLi^+ + xe^{-1} \leftrightarrow Li_{3x}Mo_{1-x}O_4 + xNi^{2+} \quad (4)$$

And the β-$NiMoO_4$ NW arrays have better conductivity than $NiMoO_4 \cdot xH_2O$ nanowires, which are beneficial to the fast electrons transfer[25, 49]. Third, from the Figure 9(c), we can see that the asymmetry supercapacitor consists of carbon rod, electrolyte, separator and β-$NiMoO_4$ NW arrays supported on carbon cloth. And the carbon rod has high conductivity and environmental friendless. Furthermore, the cylinder supercapacitor can guarantee all the β -$NiMoO_4$ NW arrays grown on carbon cloth saturated enough and easy contact between ions and electrons. Last, the β-$NiMoO_4$ NW arrays grown on carbon cloth can ensure good mechanical adhesion and enough touch between the carbon cloth and the β-$NiMoO_4$ NW arrays. It is emphasized that it can be used to fabricate solid-state supercapacitor devices, and one hybrid device could light a light-emitting diode (LED) for 260 seconds, as is shown in Figure 9(d). The charging curve is shown in Figure S3(d) and the screen is displayed in S4.

4. Conclusions

In summary, β-$NiMoO_4$ NW arrays grown on carbon cloth have been synthesized through hydrothermal method. This material is characterized by XRD, EDS, BET, SEM and TEM. The asymmetry cylinder solid supercapacitor was fabricated. This structure shows outstanding electrochemical performance with the largest specific capacitance of 414.7 F/g at the current density of 0.25 A/g, the highest energy density of 36.86 Wh/kg at power density of 100 W/kg and the maximum power density of 1100 W/kg at energy density of 12.3 Wh/kg. It remains 65.9 % of its initial capacitance after 6000 cycles. It is emphasized that it can be used to fabricate solid-state supercapacitor device, and one hybrid device could light a light-emitting diode (LED) for 260 seconds. The whole evidences prove that the β-$NiMoO_4$ nanostructure have high potential for the next generation high performance electrochemical supercapacitor.

Acknowledgements

This work has been funded by the NSFC (11204388), the SRFDP (20120191120039), the NSFCQ (cstc2014jcyjA50030), the Development Program ("863" Program) of China (2015AA034801), the Fundamental Research Funds for the Central Universities (No.CQDXWL-2014-001, No.CQDXWL-2013-012, No.106112015CDJXY300004), and the large-scale equipment sharing fund of Chongqing University.

References

1. P. Yang, W. J. Mai, Nano Energy. 2014, **8**, 274.
2. S. G. Dai,Y. Xi, C. G. Hu, B. S. Hu, X.L. Yue, L. Cheng, G. Wang.RSC Adv. 2014, 4, 40542.
3. M. Beidaghi and Y.Gogotsi, Energy Environ. Sci. ,2014, **7**, 867.
4. S. E. Moosavifard, J. Shamsi, S. Fani and S. Kadkhodazade, RSC Adv., 2014, 4, 52555.
5. C. Liu, F. Li, L.P. Ma, H.M. Cheng, Adv.Mater. 2010, **22**, E28.
6. S. E. Moosavifard, J. Shamsi, M. Ayazpour, Ceramics International.2015, **41**, 1831.
7. G. P. Wang, L. Zhang, J. J. Zhang, Chem. Soc. Rev. 2012, **41**, 797.
8. P. Simon, Y. Gogotsi, Nat.Mater. 2008, **7**, 845.
9. C. Liu, F. Li, L. P. Ma, H. M. Cheng, Adv. Mater.2010, **22**, E28.
10. P. Simon, Y. Gogotsi , Nat.Mater. 2008, **11**, 845.
11. H. Jiang, P. S. Lee, C. Li, Energy Environ. Sci. 2013, **6**, 41.
12. M.D. Stoller, R.S. Ruoff, Energy Environ. Sci. 2010, **3**, 1294.
13. J. Bae, M. K. Song, Y. J. Park, J. M. Kim, M. Liu and Z. L. Wang, Angew. Chem. Int. Ed. 2011, **50**, 1683.
14. Z. Weng, Y. Su, D. W. Wang, F. Li, J. Du and H. M. Cheng, Adv. Energy Mater. 2011, **1**, 917.
15. V. Khomenko, E. Raymundo-Pinero and F. Beguin, J. Power Sources.2006, **153**, 183.
16. L. Demarconnay, E. Raymundo-Pinero and F. Beguin, J.Power Sources. 2011, **196**, 580.
17. C. Yuan, J. Li, L. Hou, L. Yang, L. Shen, X. Zhang, Electrochim. Acta. 2012, **78**, 532.
18. F. Zhang, C. Yuan, X. Lu, L. Zhang, Q. Che, X. Zhang, J. Power Sources. 203 2012, **203**, 250.
19. M. J. Deng, J. K. Chang, C. C. Wang, K.W. Chen, C. M. Lin, M.T. Tang, J. M. Chen, K. T. Lu, Energy Environ. Sci. 2011, **4**, 3942.
20. R. Kotz, M. Chalen, Elecchemical Acta. 2000, **45**, 2482.
21. Q. Wang, X. Wang, B. Liu, G. Yu, X. Hou, D. Chen, G. Shen, J. Mater. Chem. A. 2013, **1**, 2468.
22. D. P. Cai, B. Liu, D.D. Wang, Y. Liu, L. L. Wang, L. Han, Y. R. Wang ,Electrochemical Acta.2014, **125**, 294.
23. M. C. Liu, L. B. Kong, C. Lu, X. M. Li, Y. C. Luo, L. Kang, Mater. Lett. 2013, **94**, 197.
24. J. Liu, J. Jiang, C. Cheng, H. Li, J. Zhang, H. Gong, H.J. Fan, Adv. Mater. 2011, **23**, 2076.
25. L. Yu, G. Zhang, C. Yuan, X.W. Lou, Chem. Commun. 2013, **49**, 137.
26. S. G. Dai, Y. Xi, C. G. Hu, X. L. Yue, L. Cheng, G. Wang, Journal of Power Sources, 2015, **274**, 477.

27. B. Moreno, E. Chinarro, M. T. Colomer, J. R. Jurado, J. phys. Chem. C 2010, **114,** 4251.

28. J. Haetge, I. Djerdj and T. Brezesinski, Chem. Commun. 2012, **48,** 6726.

29. J. H. Ahn, G. D. Park, Y. C. Kang, J. H. Lee, Electrochimica Aca 2015, **174** , 102.

30. B. H. Qu, Y. J. Chen, M. Zhang, L. L. Hu, D. N. Lei, B.G. Lu, Q. H. Li, Y. G. Wang, L. B. Chen, T. H. Wang, Nanoscale, 2012, **4**, 7810.

31. D. Guo, Y. Z. Luo, X. Z. Yu, Q. H. Li, T. H. Wang, Nano Energy, 2014, **8**, 174.

32. J. Yan, Z. J. Fan, W. Sun, G. Q. Ning, T. Wei, Q. Zhang, R. F. Zhang, L. J. Zhi, F.Wei, Adv. Funct. Mater. 2012, **22**, 2632.

33. A. L. M. Reddy, F. E. Amitha, I. Jafri, S. Ramaprabhu, Nanoscale Res Lett. 2008, **3**, 145.

34. A. S. Adekunle, B. O. Agboola, K. I. Ozoemena, E. E. Ebenso, J. A.O. Oyekunle, O. S. Oluwatobi, J. N. Lekitima. Int. J. Electrochem. Sci., 2015, **10**, 3414.

35. G. K. Veerasubramani, K. Krishnamoorthy, R. Sivaprakasam, S. J. Kim.,Mat.Chem.and phy., 2014, **147**, 836.

36.T. Yang, H. Zhang, Y. Z. Luo, L. Mei, D. Guo, Q. L. Li, Electrochimica Acta, 2015, 158, 327.

37. A. Klein, P. Axmann, C. Yada, M. W. Mehrens, JPS., 2015, **288**,302.

38. M.C. Liu, L. Kang, L.B. Kong, C. Lu, X.J. Ma, X.M. Li, Y.C. Luo, RSC Advances. 2013, **3**, 6472.

39.D. P. Cai, D. D. Wang, B. Liu, Y. R. Wang, Y. Liu, L. L. Wang, H. Li, H. Huang, Q. H. Li, and T. H. Wang. ACS APPLIED MAT. 2013, **5**, 12905.

40. W. Hong, J.Q. Wang, P.W. Gong, J. F. Sun, L. Y. Niu, Z. G. Yang, Z. F. Wang, S. R. Yang, JPS.,2014, **270**, 516.

41. L. Y. Yuan, X. H. Lu, X Xiao, T Zhai, J. J. Dai, F. C. Feng, B. Hu, X. Wang, L. Gong, J. Chen, C. G. Hu, Y. X. Tong, J. Zhou, and Z. L. Wang. ACS NANO. 2012, **6**, 656.

42. M. C. Liu, L. Kang, L. B. Kong, C. Lu, X. J. Ma, X. M. Li and Y. C. Luo. RSC Adv. 2013, **3**, 6472.

43.M.Q. Xue, Z. Xie, L. S. Zhang, X. L. Ma, X. L. Wu, Y. G. Guo, W. G. Song, Z. B. Li and T. B. Cao,Nascale, 2011, **3**, 2703.

44.R. S. Ray, B. Sarma, M. Misra, Materials lett., 2015, **155**, 102.

45.B. M. Sanchez, T. Brousee, C. R. Castro, V. Nicolosi, P. S. Grant, Electrochimica Acta, 2013, **91**, 253.

46 G. Wang, L. Zhang, J. Zhang, Chem. Soc. Rev. 2012, **41**, 797.

47. S. Chen, W. Xing, J. Duan, X. Hu, S.Z. Qian, J. Mater. Chem. A. 2013, **1**, 2941.

48. K.K.Purushothaman, M. Cuba, G. Muralidharan, Materials Research Bulletin, 2012, **47**, 3348.

49. B. Moreno, E. Chinarro, M.T. Colomer, J.R. Jurado, J. Phys. Chem.C. 2010, **114**, 4251.

Figure Caption

Fig. 1 Schematic illustration for the formation processes of the β-$NiMoO_4$ NW arrays on carbon cloth

Fig. 2 (a) XRD patterns of β-$NiMoO_4$ NW arrays (b) EDS patterns of the products (c) TEM low resolution image of the pure β-$NiMoO_4$ NW arrays (d) Typical TEM high resolution image of the β-$NiMoO_4$ NW arrays

Fig. 3 SEM images of perpared the β-$NiMoO_4$ NW arrays on carbon cloth(a), (b), (c）at different hours at 140 ℃（5, 8, and 11 h）and (d) SEM image of the β-$NiMoO_4$ NW arrays at 180 ℃.

Fig. 4 Schematic illustration of the 3D solid supercapacitor

Fig. 5 Electrochemical characterizations of the β-$NiMoO_4$ NW arrays grown on carbon cloth CV curves of (a), (b), (c) at various scan rates on different reaction hours (5, 8 and 11 h) and CV curve of (b) at the scan rate of 200 mV/s.

Fig. 6 Electrochemical characterizations of the β-$NiMoO_4$ NW arrays grown on carbon cloth (a) Galvanostatic charge-discharge curves for 3D solid asymmetry ECs at current density of 0.75 A/g with different reaction time. (b) Galvanostatic charge-discharge curves for 3D solid asymmetry ECs at different current densities (c) The specific capacitance at different current densities. (d) Ragon plot for 3D solid asymmetry ECs

Fig. 7 Cycling stability of β-$NiMoO_4$ NW arrays supported on carbon cloth at current density of 6 A/g and the Columbic effencicy over 6000 cycles.

Fig. 8 (a) Nyquist plot impedance from 1 to 100 kHz, inset is the corresponding equivalent electrical circuit and enlarged semicircle.(b) EIS spectra of device at first cycle and 6000th cycle.

Fig. 9 Schematic illustration for the performance of β-$NiMoO_4$ NW arrays

1

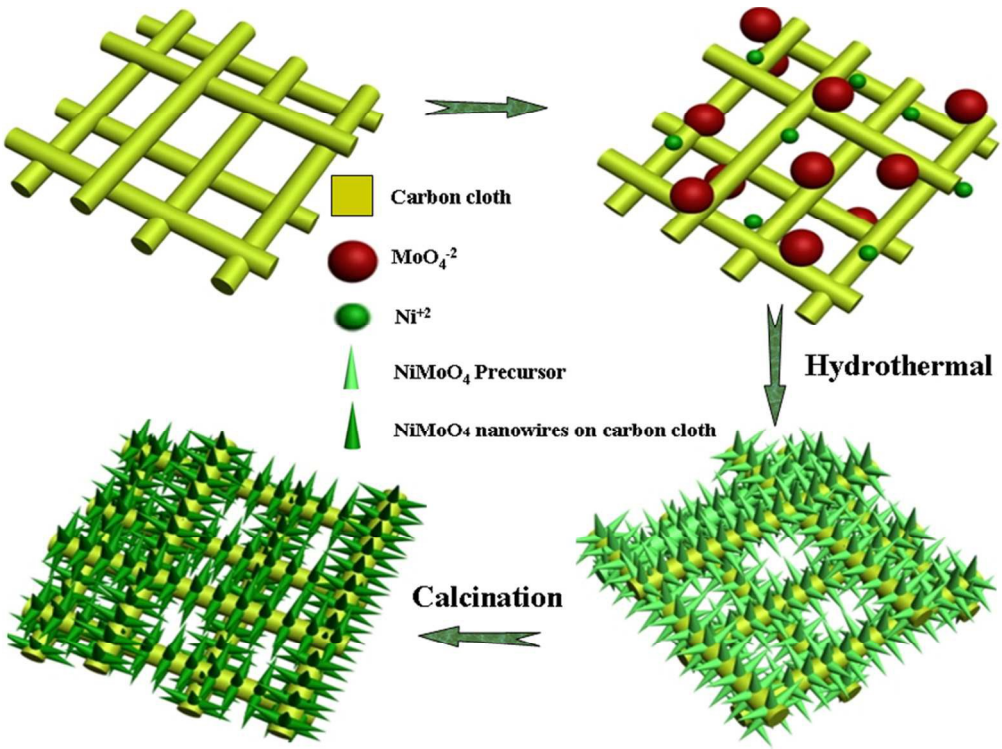

Schematic illustration for the formation processes of the β-NiMoO4 NW array on carbon cloth
85x62mm (300 x 300 DPI)

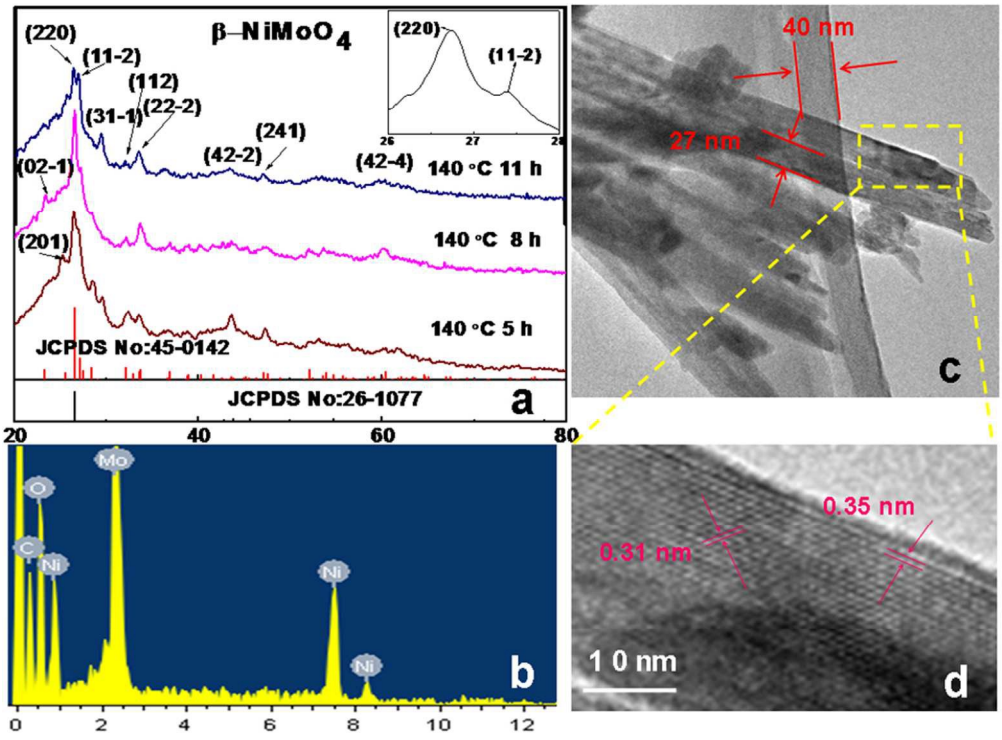

85x61mm (300 x 300 DPI)

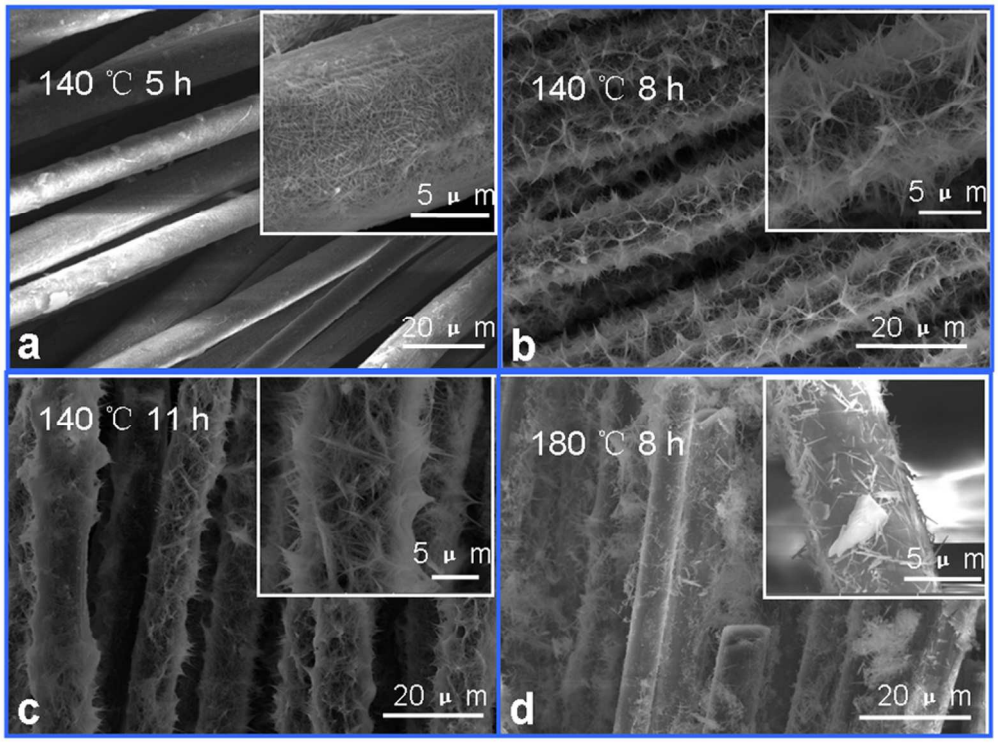

85x63mm (300 x 300 DPI)

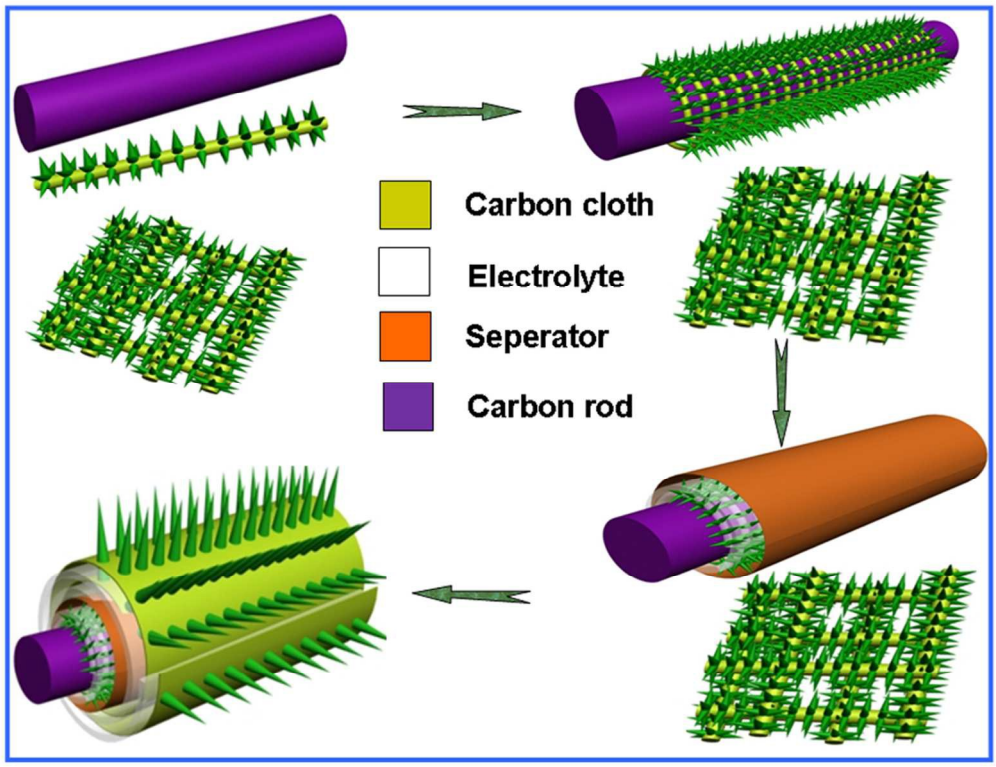

85x65mm (300 x 300 DPI)

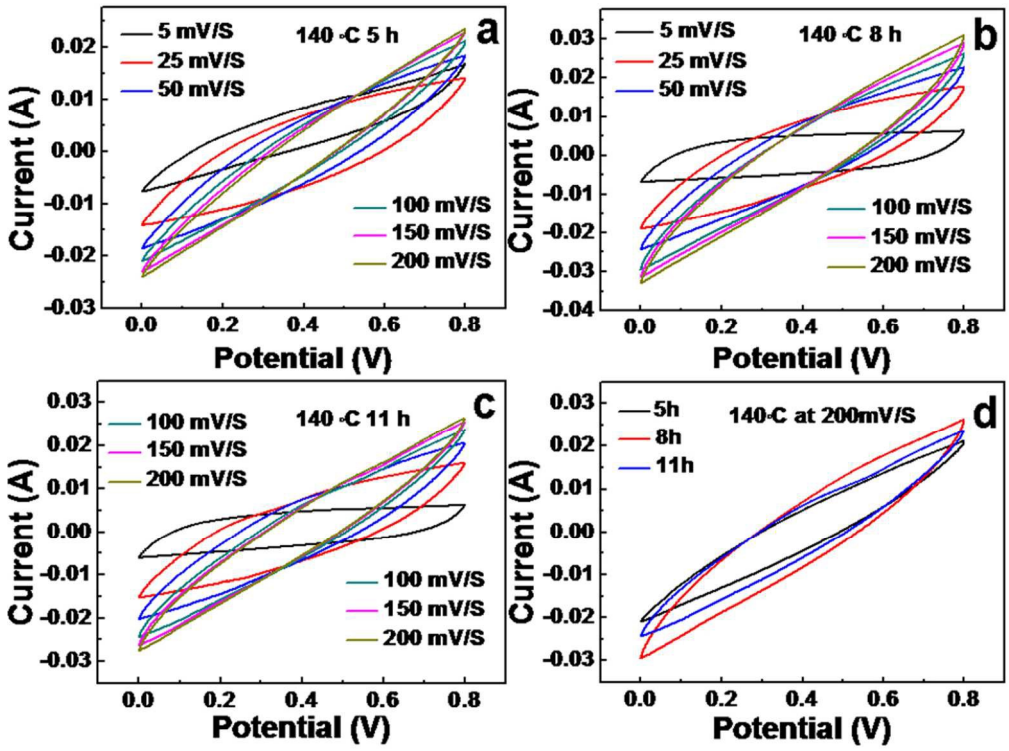

85x63mm (300 x 300 DPI)

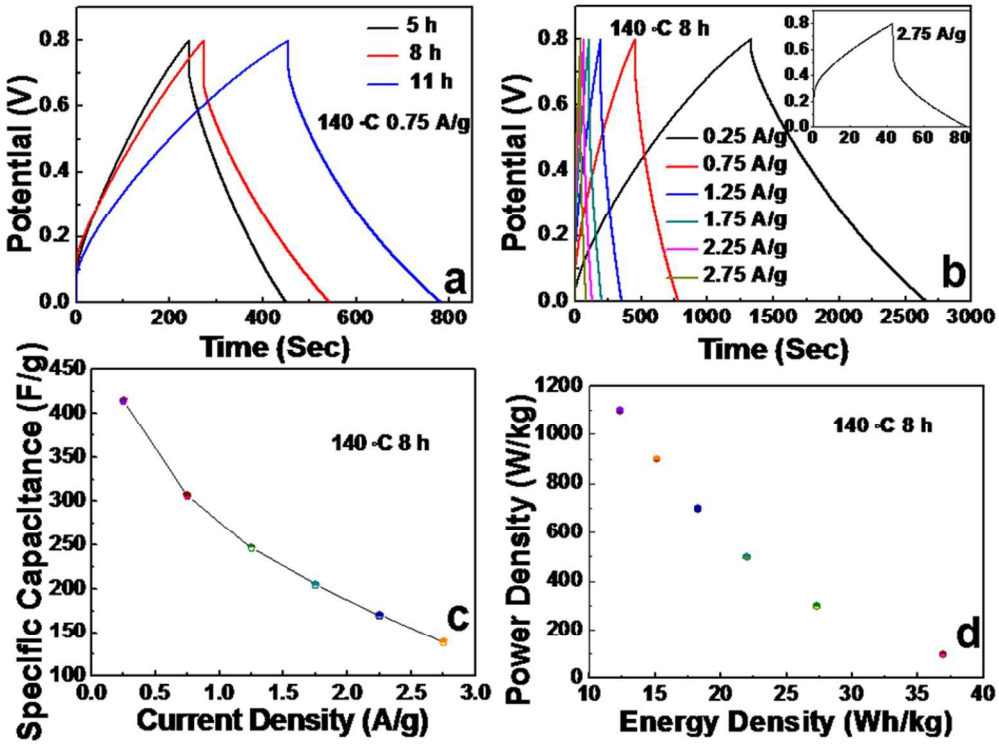

85x62mm (300 x 300 DPI)

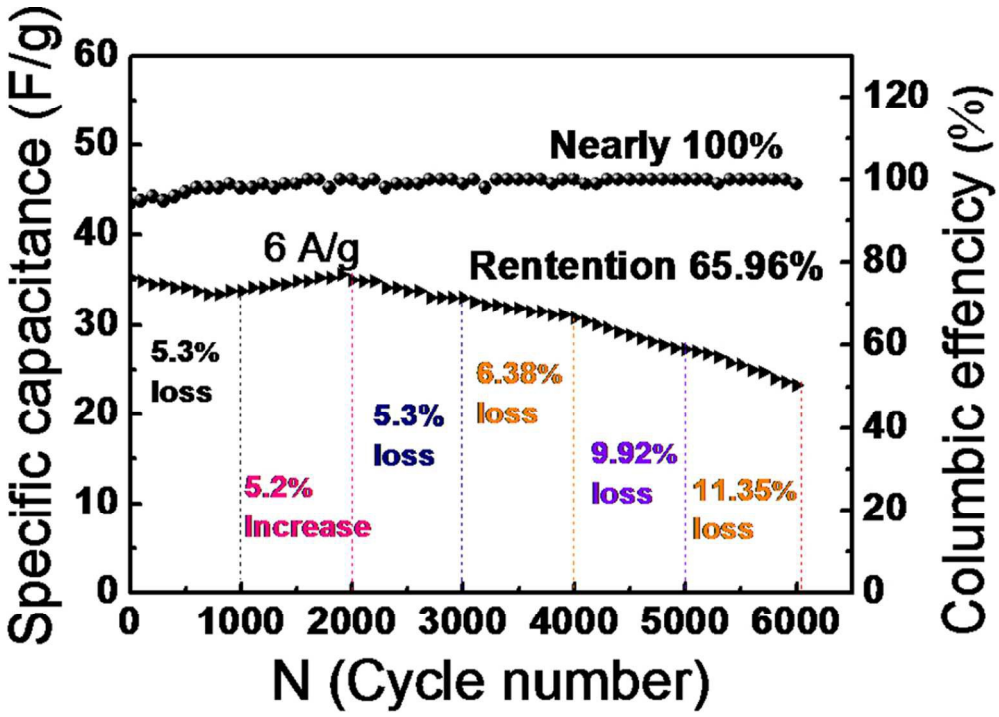

85x60mm (300 x 300 DPI)

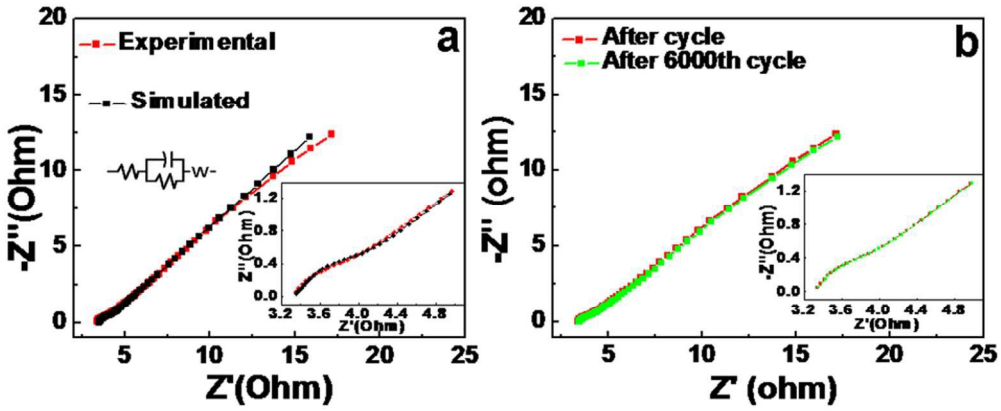

85x34mm (300 x 300 DPI)

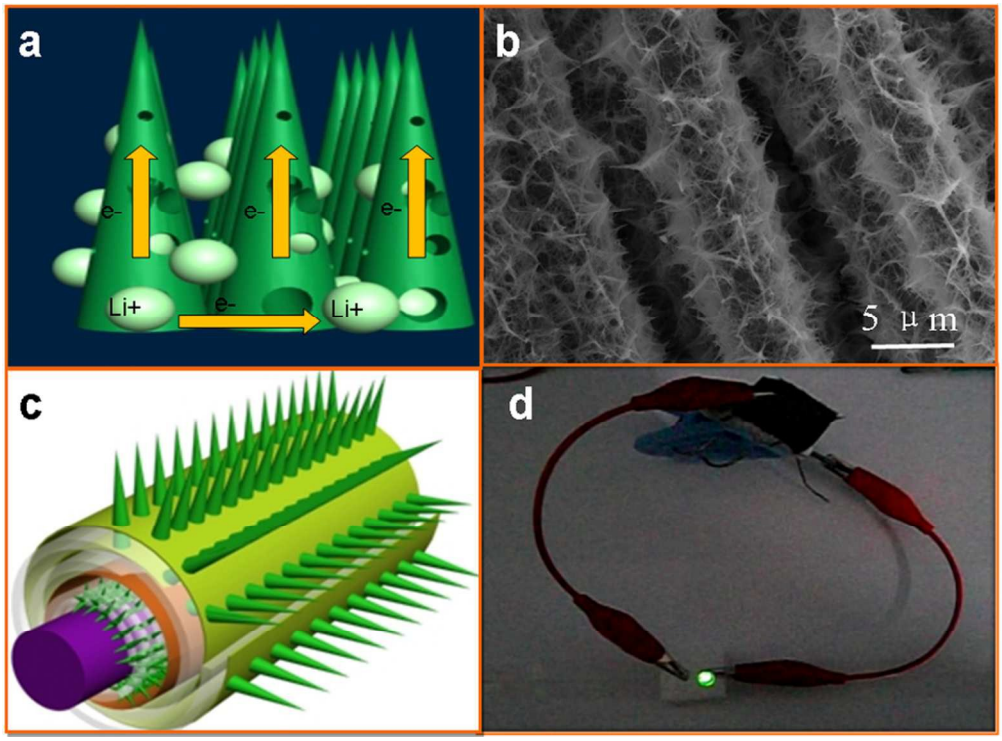

85x62mm (300 x 300 DPI)

MS Title: **β-NiMoO4 nanowire arrays grown on carbon cloth for 3D solid asymmetry supercapacitor**

Author: Chuanshen Wang, Yi Xi, Chenguo Hu, Shuge Dai, Mingjun Wang, Lu Cheng, Weina Xu, Guo Wang and Wenlong Li

Corresponding author: Yi Xi, Department of Applied Physics, Chongqing University, Chongqing, 400044, China, Tel: 086-23-65678362, Fax: 086-23-65678262
E-mail: yxi6@cqu.edu.cn

Graphical Abstract

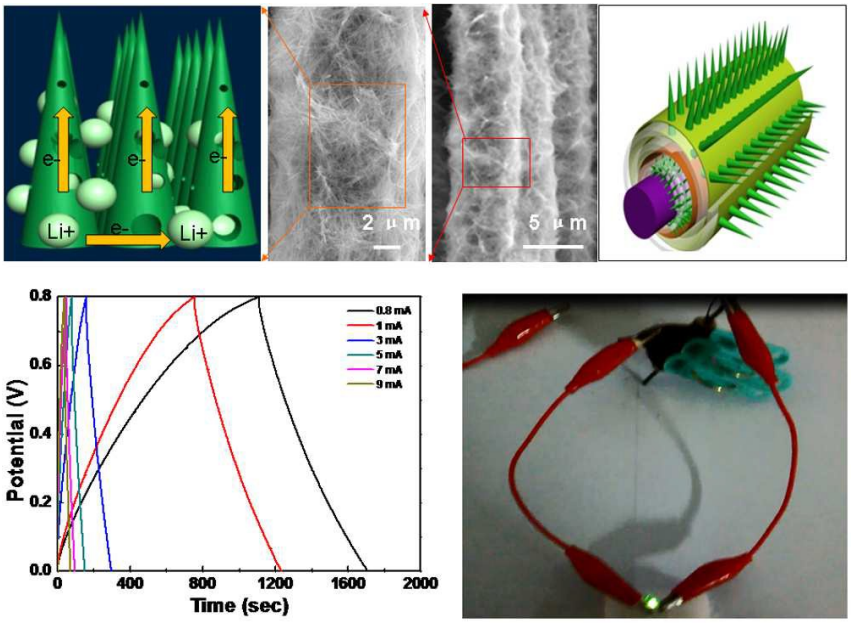

One β-$NiMoO_4$ NWs supercapacitor to light one light-emitting diode (LED) for 260 seconds and it can deliver larger specific capacitance (546 F/g at scan rate of 5 mV/s), higher energy density (30.92 Wh/kg), the maximum power density of 2831 W/kg and cycling stability (86.6 % capacity retention after 1500 cycles).